

Color Variability of Asteroids in SDSS Moving Object Catalog

Gy. M. Szabó^{1,2*}, Ž. Ivezić^{3,4}, M. Jurić³, R. Lupton³ and L. L. Kiss^{1,5}

¹*Department of Experimental Physics & Astronomical Observatory, University of Szeged, 6720 Szeged, Hungary*

²*Department of Physics and Astronomy, Johns Hopkins University, Baltimore, MD, 21218*

³*Princeton University Observatory, Princeton, NJ 08544*

⁴*H.N. Russell Fellow*

⁵*University of Sydney, School of Physics, Sydney, Australia*

ABSTRACT

We report a detection of statistically significant color variations for a sample of 7,531 multiply observed asteroids that are listed in the Sloan Digital Sky Survey Moving Object Catalog. Using 5-band photometric observations accurate to ~ 0.02 mag, we detect color variations in the range 0.06-0.11 mag (rms). These variations appear uncorrelated with asteroids physical characteristics such as diameter (in the probed 1-10 km range), taxonomic class, and family membership. Despite such a lack of correlation, which implies a random nature for the cause of color variability, a suite of tests suggest that the detected variations are not instrumental effects. In particular, the observed color variations are incompatible with photometric errors, and, for objects observed at least four times, the color change in the first pair of observations is correlated with the color change in the second pair. These facts strongly suggest that the observed effect is real, and also indicate that for some asteroids color variations are larger than for others. The detected color variations can be explained as due to inhomogeneous albedo distribution over an asteroid surface. Although relatively small, these variations suggest that fairly large patches with different color than their surroundings exist on a significant fraction of asteroids. This conclusion is in agreement with spatially resolved color images of several large asteroids obtained by NEAR spacecraft and HST.

Key words:

1 INTRODUCTION.

Asteroids are rotating aspherical reflective bodies which thus exhibit brightness variations. As recognized long ago (Russell 1906, Metcalf 1907), studies of their lightcurves provide important constraints on their physical properties, and processes that affect their evolution. For example, well-sampled and accurate lightcurves can be used to determine asteroid asphericity, spin vector, and even the albedo inhomogeneity across the surface (Magnusson 1991). The current knowledge about asteroid rotation rates and lightcurve properties is well summarized by Pravec & Harris (2000). The rotational periods range from ~ 2 hours to ~ 15 hours. The lightcurve amplitudes for main-belt asteroids and near-Earth objects are typically of the order 0.1-0.2 mag. (peak-to-peak). Recently, similar variations have been detected for a dozen Kuiper Belt Objects (Sheppard & Jewitt 2002). The largest amplitudes of ~ 2 mag. (peak-to-peak) are observed for as-

teroids 1865 Cerberus and 1620 Geographos (Wisniewski et al. 1997, Szabó et al 2001).

In contrast to appreciable and easily detectable amplitudes of single-band light curves, typical asteroid color variations are much smaller. Indeed, if albedo didn't vary across an asteroid's surface, then the asteroid would not display color variability irrespective of its geometry¹ While the absence of color variability may also be consistent with a gray albedo variation, the strong observed correlation between asteroid albedo and color (blue C type asteroids have visual albedo of $p_V \sim 0.04$, while for red S type asteroids $p_V \sim 0.15 - 0.20$, Zellner 1979, Shoemaker et al. 1979) implies that non-uniform albedo distribution should be detectable through color variability. Following Magnusson (1991), hereafter we will refer to non-uniform albedo distribution across an asteroid surface as to albedo variegation.

* E-mail: szgy@mcse.hu

¹ Apart from the so-called differential albedo effect (Bowell & Lumme, 1979).

The most notable case of albedo variegation is displayed by 4 Vesta which apparently has one bright and one dark hemisphere (Blanco & Catalano 1979; Degewij, Tedesco & Zellner 1979, Binzel et al. 1997). Definite color variations have been detected in only a few dozen asteroids. A color variability at the level of a few percent has been measured directly for Eros (V-R and V-I, Wisniewski 1976) and for 51 Nemausa (u-b, v-y, Kristensen & Gammelgaard 1993). In a study that still remains one of the largest monitoring programs for color variability, Degewij, Tedesco & Zellner (1979) detected color variations greater than 0.03 mag. in 6 out of 24 monitored asteroids. In another notable study, Schober & Schroll (1982) detected color modulation in 49 asteroids. Recently, a spectacular confirmation of albedo variegation has been obtained for Eros by NEAR multispectral imaging (Murchie et al. 2002). While similar spatially resolved images are available for several other objects (e.g. Zellner et al. 1997, Binzel et al. 1997, Baliunas et al. 2003), the number of asteroids with observational constraints on their albedo variegation remains small.

Here we study asteroid color variability by utilizing the Sloan Digital Sky Survey Moving Object Catalog (hereafter SDSSMOC, Ivezić et al. 2002a). SDSSMOC currently contains accurate (0.02 mag) 5-band photometric measurements for over 130,000 asteroids. A fraction of these objects are previously recognized asteroids with available orbits, and 7,531 of them were observed by SDSS at least twice. We use the color differences between the two observations of the same objects to constrain the ensemble properties, as opposed to studying well-sampled light curves for a small number of objects. The lack of detailed information for individual objects is substituted by the large sample size which allows us to study correlations between color variability and various physical properties in a statistical sense. Also, objects in the sample studied here have typical sizes 1–10 km, about a factor 10 smaller than objects for which color variations have been reported in the literature.

We describe the SDSSMOC and data selection in Section 2, and in Section 3 we perform various tests to demonstrate that detected color variability of multiply observed objects is not an observational artefact. In Section 4 we search for correlations between the color variability and asteroid physical properties, and summarize our results in Section 5.

2 SDSS OBSERVATIONS OF MOVING OBJECTS

SDSS is a digital photometric and spectroscopic survey which will cover 10,000 deg² of the Celestial Sphere in the North Galactic cap and a smaller (~ 225 deg²) and deeper survey in the Southern Galactic hemisphere (Azevajian et al. 2003, and references therein). The survey sky coverage will result in photometric measurements for about 50 million stars and a similar number of galaxies. About 50% of the Survey is currently finished. The flux densities of detected objects are measured almost simultaneously in five bands (Fukugita et al. 1996; u , g , r , i , and z) with effective wavelengths of 3551 Å, 4686 Å, 6166 Å, 7480 Å, and 8932 Å, 95% complete for point sources to limiting magnitudes of 22.0, 22.2, 22.2, 21.3, and 20.5 in the North Galactic cap.

Astrometric positions are accurate to about 0.1 arcsec per coordinate (rms) for sources brighter than 20.5^m (Pier et al. 2002), and the morphological information from the images allows robust star-galaxy separation (Lupton et al. 2001) to $\sim 21.5^m$.

SDSS, although primarily designed for observations of extragalactic objects, is significantly contributing to studies of the solar system objects, because asteroids in the imaging survey must be explicitly detected to avoid contamination of the samples of extragalactic objects selected for spectroscopy. Preliminary analysis of SDSS commissioning data (Ivezić et al. 2001, hereafter I01) showed that SDSS will increase the number of asteroids with accurate five-color photometry by more than two orders of magnitude, and to a limit about five magnitudes fainter (seven magnitudes when the completeness limits are compared) than previous multi-color surveys (e.g. The Eight Color Asteroid Survey, Zellner, Tholen & Tedesco 1985).

2.1 The Sample Selection Using SDSS Moving Object Catalog

SDSS Moving Object Catalog² is a public, value-added catalog of SDSS asteroid observations. In addition to providing SDSS astrometric and photometric measurements, all observations are matched to known objects listed in the ASTORB file (Bowell 2001), and to the database of proper orbital elements (Milani et al. 1999), as described in detail by Jurić et al. (2002, hereafter J02). Multiple SDSS observations of objects with known orbital parameters can be accurately linked, and thus SDSSMOC contains rich information about asteroid color variability.

We select 7,531 multiply observed objects from the second SDSSMOC edition (ADR2.dat) by requiring that the number of observations (N_{ap}) is at least two, and use the first and second observations to compute photometric changes. A “high-quality” sample of 2,289 asteroids is defined by two additional restrictions:

- In order to avoid the increased photometric errors at the faint end, we require $r < 19$.
- In order to minimize the effect of variable angle from the opposition on the observed color, we select only objects for which the change of this angle is less than 1.5 degree.

We also utilize a subsample of 541 asteroids that were observed at least four times.

Since SDSS observations of asteroids are essentially random, and the time between them (days to months, 75% of repeated observations are obtained within 3 months, and 86% within a year) is much longer than typical rotational periods (< 1 day), the phases of any two repeated observations are practically uncorrelated. Thus, the distribution of magnitude and color changes for a large ensemble of asteroids is a good proxy for random two-epoch sampling of an asteroid’s single-band and color lightcurves. Of course, this is strictly true only if the distributions of amplitudes and shapes of these light curves are fairly narrow. For wide

² Available at <http://www.sdss.org>

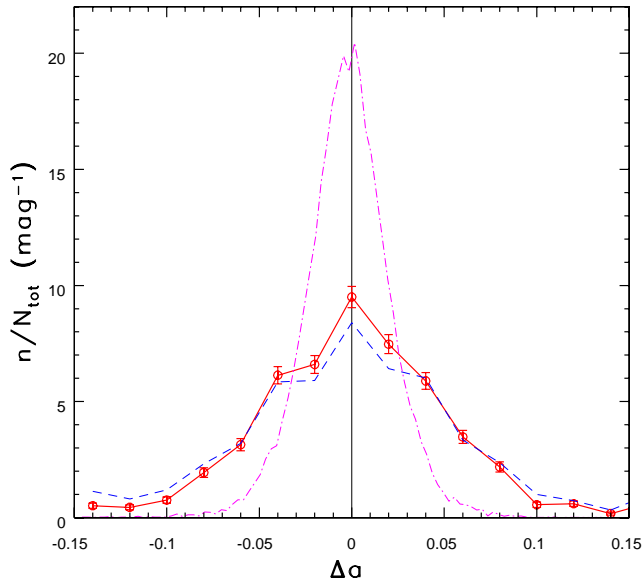


Figure 1. The dashed line shows the distribution of the a color change between two epochs for all 7,531 asteroids from SDSS-MOC that were observed at least twice. The symbols with error bars connected by the solid line show the distribution of the a color change for a subset of 2,289 asteroids brighter than $r = 19$ and with the difference in angles from the opposition smaller than 1.5 degree. Its equivalent Gaussian width, determined from the interquartile range, is 0.053 mag. The dash-dotted line shows the distribution of the a color change between two epochs for 21,000 stars brighter than $r = 19$. Its width, which indicates the measurement error for a color, is 0.023 mag.

distributions of amplitudes and shapes, the observed two-epoch magnitude and color changes represent convolution of the two effects.

3 ASTEROID COLOR VARIABILITY IN SDSSMOC

The colors of asteroids in SDSS photometric system are discussed in detail by I01. They defined a principal color in the $r - i$ vs. $g - r$ color-color diagram, a , as

$$a \equiv 0.89(g - r) + 0.45(r - i) - 0.57. \quad (1)$$

The a color distribution is strongly bimodal (see Fig. 9 in I01), with the two modes at -0.1 and 0.1 . The rms scatter around each mode is about 0.05 mag. The two modes are associated with different taxonomic classes: the “blue” mode includes C, E, M and P types, and the “red” mode includes S, D, A, V and J types (see Fig. 10 in I01). The Vesta type asteroids (type V) can be effectively separated from “red” asteroids using the $i - z$ color (J02). The a and $i - z$ colors are strongly correlated with dynamical family membership (Ivezić et al. 2002c, hereafter I02c). Hereafter, we chose the a color as the primary quantity to study asteroid color variability.

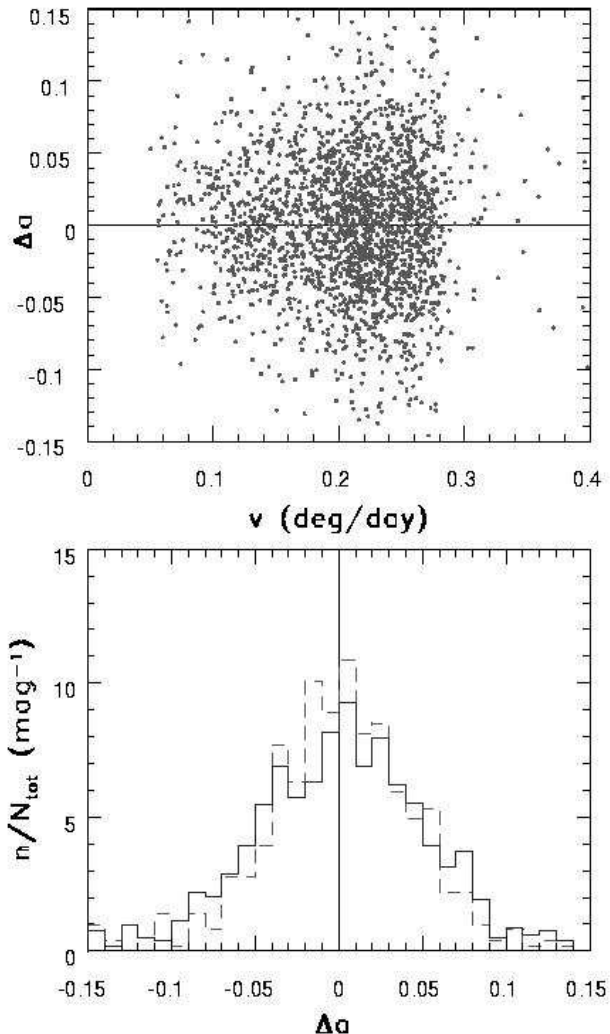


Figure 2. The upper panel shows the a color change between two epochs for the same asteroids as in Fig. 1, as a function of the object’s velocity. The bottom panel compares the width of the distribution of the a color change for 511 objects with $0.10 < v < 0.18$ (dashed line) and for 1,065 objects with $v > 0.22$ deg/day (solid line). Note that the two histograms are statistically indistinguishable indicating that the color measurement is not affected by the object’s apparent velocity.

3.1 Detection of Asteroid Color Variability in SDSSMOC

The observed distribution of the a color change between two epochs, Δa , for 2,289 selected asteroids, is shown by symbols (with error bars) in Figure 1. Its equivalent Gaussian width determined from the interquartile range (hereafter “width”), is 0.053 mag. The expected width based on the formal errors reported by the SDSS photometric pipeline (“photo”, Lupton et al. 2001) is 0.02 mag., indicating that the observed Δa distribution reflects intrinsic asteroid color changes. However, the formal errors may not be correct. In order to determine the measurement accuracy for the a color, we use 21,000 stars with $r < 19$ that were observed twice. The dashed line in Figure 1. shows their Δa distribu-

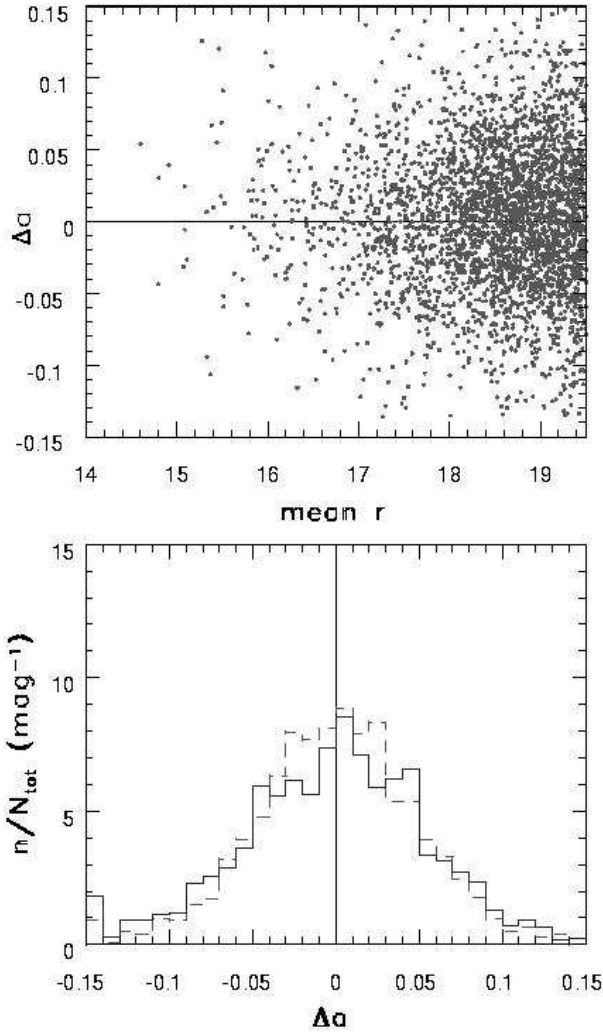


Figure 3. The upper panel shows the a color change between two epochs for the same asteroids as in Fig. 1, as a function of the object’s apparent magnitude. The bottom panel compares the width of the distribution of the a color change for 214 objects with $r < 17$ (dashed line) and for 898 objects with $18.5 < r < 19$ (solid line). Note that the two histograms are statistically indistinguishable indicating that the color measurement is not affected by the object’s apparent magnitude.

tion. Its width is 0.023 mag., in agreement with the expectations based on formal errors.

Subtracting the error distribution width of 0.023 mag. in quadrature, the intrinsic a color root-mean-square (rms) variation is 0.04 mag. While Fig.1 demonstrates that this measurement is statistically highly significant, in the remainder of this section we test for the presence of spurious observational effects that could be responsible for the observed asteroid color variation.

3.2 Tests for Spurious Observational Effects

3.2.1 Color Change vs. Asteroid’s Velocity

Although the formal photometric errors for stars are correct, asteroids move during observations and their motion could

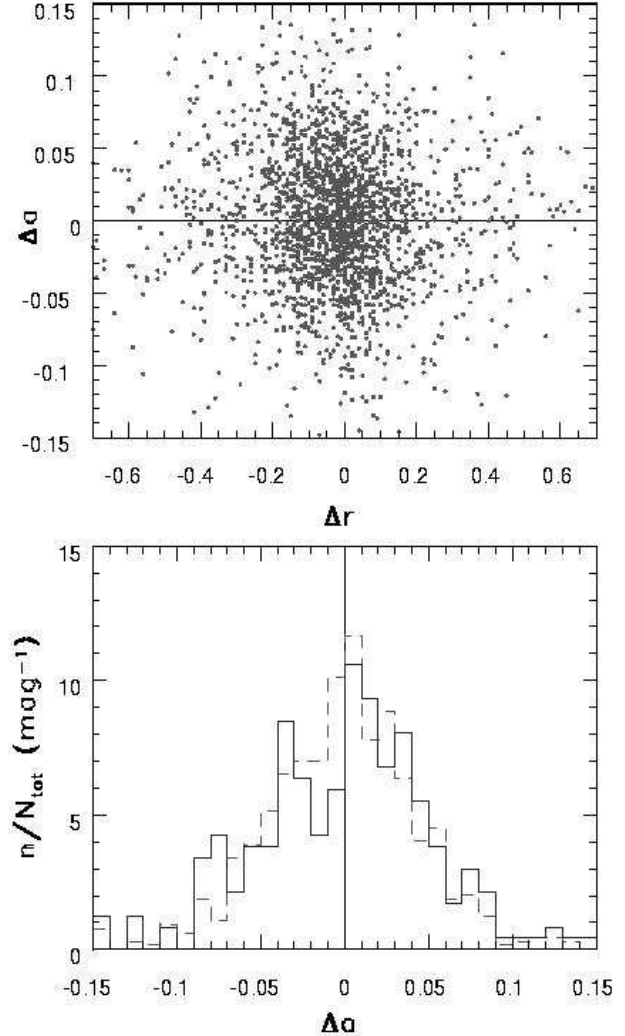


Figure 4. The upper panel shows the a color change between two epochs for the same asteroids as in Fig. 1, as a function of the change in the r band apparent magnitude. The bottom panel compares the width of the distribution of the a color change for 645 objects with $|\Delta(r)| < 0.05$ (dashed line) and for 1,644 objects with $|\Delta(r)| > 0.05$ (solid line). Note that the two histograms are statistically indistinguishable indicating that the color measurement is not correlated with the change of the object’s apparent magnitude.

in principle affect the photometric accuracy. While this effect should be negligible (the images are not strongly trailed), we test for it by correlating Δa with the object’s velocity. If the photometric accuracy is lower for moving objects, the Δa distribution width should increase with magnitude of the object’s velocity. The Δa vs. v diagram is shown in the top panel in Figure 2. The bottom panel compares the width of the Δa distribution for two subsamples selected by velocity. The dashed line shows the Δa distribution for 511 objects with $0.1 \text{ deg/day} < v < 0.18 \text{ deg/day}$, and the solid line for 1,065 ones with $v > 0.22 \text{ deg/day}$. As evident, the two histograms are statistically indistinguishable.

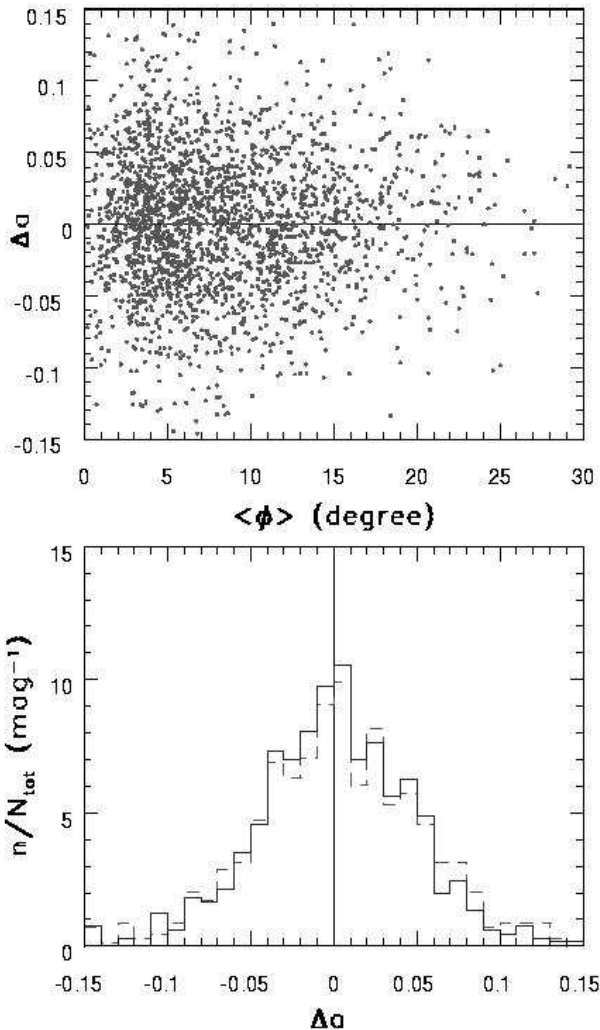


Figure 5. The upper panel shows the a color change between two epochs for the same asteroids as in Fig. 1, as a function of the mean angle from the opposition. The bottom panel compares the width of the distribution of the a color change for 712 objects with $\phi < 5^\circ$ (dashed line) and for 664 objects with $10^\circ < \phi < 20^\circ$ (solid line). Note that the two histograms are statistically indistinguishable indicating that the color measurement is not correlated with the mean angle from the opposition.

3.2.2 Color Change vs. Apparent Brightness

The photometric errors typically increase with apparent magnitude of the measured object. While the adopted faint limit ($r < 19$) is sufficiently bright that SDSS photometric errors are nearly independent of magnitude (Ivezić et al. 2002c), we test this expectation by correlating Δa with the mean apparent magnitude in Fig. 3. The bottom panel compares the width of the Δa distribution for two subsamples selected by $r < 17$ (dashed line, 214 objects) and by $18.5 < r < 19$ (solid line, 898 objects). There is no significant difference between the two histograms. Relaxing the magnitude cut to $r < 20$ yields the same null result with an increased sample size by a factor of 2. We have also tested Δa vs. Δr dependence, illustrated in Fig. 4, and did not detect any correlation.

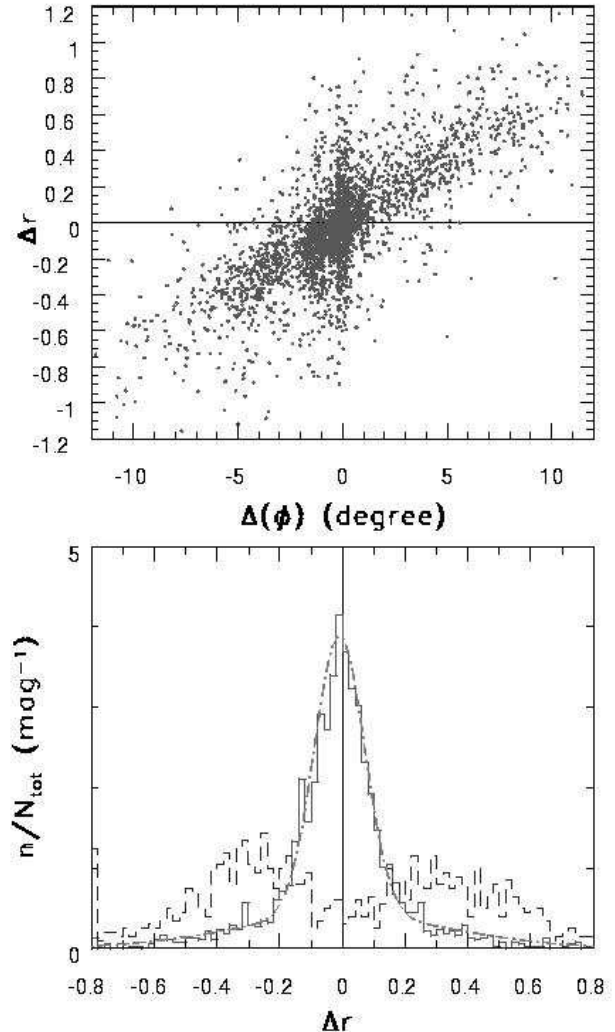


Figure 6. The upper panel shows the change of r magnitude for the full sample, as a function of the change of the angle from the opposition. The bottom panel compares the Δr distributions for two ranges of the angle change: $0^\circ - 1^\circ$ as the solid line and $2^\circ - 10^\circ$ as the dashed line. The former is well fit by a sum of two Gaussians (see text) shown as the dash-dotted line.

3.2.3 Color Change vs. the Angle from the Opposition

In order to minimize the opposition effect (see Section 6.1 in I01), the maximum change of the angle from the opposition (between two observations) in the analyzed sample is constrained to 1.5 deg (this limit may be slightly too conservative since we find no correlation between Δa and the change of the angle from the opposition for changes as large as 10°). To exclude the possibility that the color change is affected by the *mean* angle from the opposition, we analyze Δa as a function of this angle in Fig. 5. There is no discernible correlation.

Unlike the color change which is not correlated with the angle from the opposition, the change of magnitudes between two epochs is strongly correlated with this angle, as expected. The top panel in Fig. 6 shows the dependence of Δr on the change of the angle from the opposition. The comparison of Δr distributions for two ranges of the angle

change ($0^\circ - 1^\circ$ as the solid line and $2^\circ - 10^\circ$ as the dashed line) are shown in the bottom panel. As evident, even when asteroids are observed at practically the same position, Δr has a wide distribution, mostly due to asteroid rotation. We find that the Δr distribution can be well fit by a sum of two Gaussians with the widths of 0.08 mag and 0.35 mag and amplitude ratio 2:1, shown as the dash-dotted line. The measured Δr distribution can be used to constrain the distributions of asteroid axes ratios and rotational periods. Such an analysis, while interesting in its own right, is beyond the scope of this paper.

3.2.4 The Effects of Non-simultaneous Measurements

The SDSS photometric measurements are obtained in the order r-i-u-z-g, and the elapsed time between the first (r) and last (g) measurement is ~ 5 minutes. The asteroid brightness variation during this time, even if achromatic, introduces a bias in the color measurement. For example, if an asteroid is observed during the rising part of its lightcurve, the $r - i$ color is biased red, and the $g - r$ color is biased blue. Also, due to fixed filter order, the color biases should be correlated. The expected correlations are $\Delta(g - r)/\Delta(u - g) \sim -2$, $\Delta(r - i)/\Delta(g - r) \sim -0.25$, $\Delta(i - z)/\Delta(r - i) \sim 2$, $\Delta(g - r)/\Delta(i - z) \sim -2$, $\Delta(r - i)/\Delta(u - g) \sim 0.5$, $\Delta(i - z)/\Delta(u - g) \sim 1$. With conservative assumptions that typical rotational period is as short as 2 hours, and that the peak-to-peak amplitude is as large as 0^m5 , the expected rms contribution is the largest for $g - r$ color and equal to $\sim 0^m03$, while for $r - i$ color it is less than 0^m01 .

Fig. 7 shows the six possible correlations of the four SDSS colors. The rms scatter of each color is also displayed in the figure. As evident, the variations in all four colors are too large by a factor of few to be explained by any plausible rotation parameters. Furthermore, the slopes of expected correlations, shown by the dashed lines, are not supported by the data. We conclude that the non-simultaneous nature of SDSS color measurements is not significantly contributing to the observed color variation.

The $u - g$ and $i - z$ color changes show the largest width. We have verified that imposing a magnitude cut (< 19) on the u and z magnitudes does not decrease the scatter, i.e. the large widths are not caused by the lower sensitivity of these two bands.

3.2.5 Correlated color variations

Figure 7 demonstrates that some color pairs (e.g. $\Delta(r - i)$ vs. $\Delta(g - r)$) show correlations with a slope which cannot be explained by the examined instrumental effects. We characterize the observed correlations by their linear regression, the *rms* of the fit and the linear correlation coefficient C . All the fits cross the origin (the 0th-order coefficients do not differ significantly from 0). We determined the following correlations:

$$\Delta(g - r) = -0.13(1) \cdot \Delta(u - g) \quad (2)$$

$$rms = 0.06 \quad C = -0.26$$

$$\Delta(r - i) = -0.40(2) \cdot \Delta(g - r) \quad (3)$$

$$rms = 0.06 \quad C = -0.42$$

$$\Delta(i - z) = -0.51(2) \cdot \Delta(r - i) \quad (4)$$

$$rms = 0.07 \quad C = -0.42$$

$$\Delta(i - z) = -0.13(2) \cdot \Delta(g - r) \quad (5)$$

$$rms = 0.07 \quad C = -0.12$$

There are some noteworthy aspects of this test. First, the change of $u - g$ color does not correlate with the change of $r - i$ and $i - z$ colors, although the scatter of $\Delta(u - g)$ is much higher than for the other colors. Also, the color indices $u - X$, where $X = g, r, i, z$, do not correlate with any other color index that does not include X . This is consistent with a hypothesis that the blue part of the spectrum is affected by a process which causes no color variation of the red colors.

3.2.6 The Variability Induced Motion in Color-color Diagrams

The changes of $r - i$ and $g - r$ colors, which are used to define color a , seem to be weakly correlated, with the median slope $\Delta(r - i) \sim -0.4 \Delta(g - r)$ (3). This implies that, on average, the line connecting two observations in this diagram is more aligned with the second principal axis which is perpendicular to a , than with the a axis. Using the definition of the second principal color, hereafter named p ,

$$p \equiv 0.45(g - r) - 0.89(r - i) - 0.11, \quad (6)$$

we constructed the principal color diagram shown in the top panel in Fig. 8. Note that this diagram is simply a rotated version of the $r - i$ vs. $g - r$ diagram. In this panel we simply plot the mean value of each principal color, while in the middle panel we connect two individual measurements by lines, for a small subset of objects with $18 < r < 18.3$ (to avoid crowding) and a change in each color of at least 0.03 mag. As evident, for objects with large color variations, the changes of the two principal colors seem to be somewhat correlated, with the slope larger than 1. That is, the p color varies more than the a color. In the bottom panel we show the change of p color vs. the change of a color for all the objects in the “high-quality” subsample, as well as the rms scatter in each color.

The observed variability of the p color appears nearly sufficient to explain its single-measurement distribution width of ~ 0.05 mag. (the rms width of the change in that color is 1.33 of its single-epoch width, i.e. only slightly smaller than the expected value of 1.41 if the variability was the only reason for its finite value). In order to test this hypothesis, we use a subsample of 541 asteroids that were observed at least four times. The distribution width for the mean p color, obtained by averaging the four measurements, is expected to be smaller than that measured for any individual epoch. On the other hand, no significant difference in the distribution widths is expected for the a color. The distributions shown in Fig. 9 suggest that the variability contributes significantly to the p color distribution width, and much less to the width of each individual mode in the a color distribution.

Since the variability induced motion in the p vs. a color-color diagram is more aligned with the p axis than with the a axis, over 90% of asteroids have the same a -based classification (< 0 vs. > 0) in different epochs. The same behavior also indicates that the color variability cannot be explained

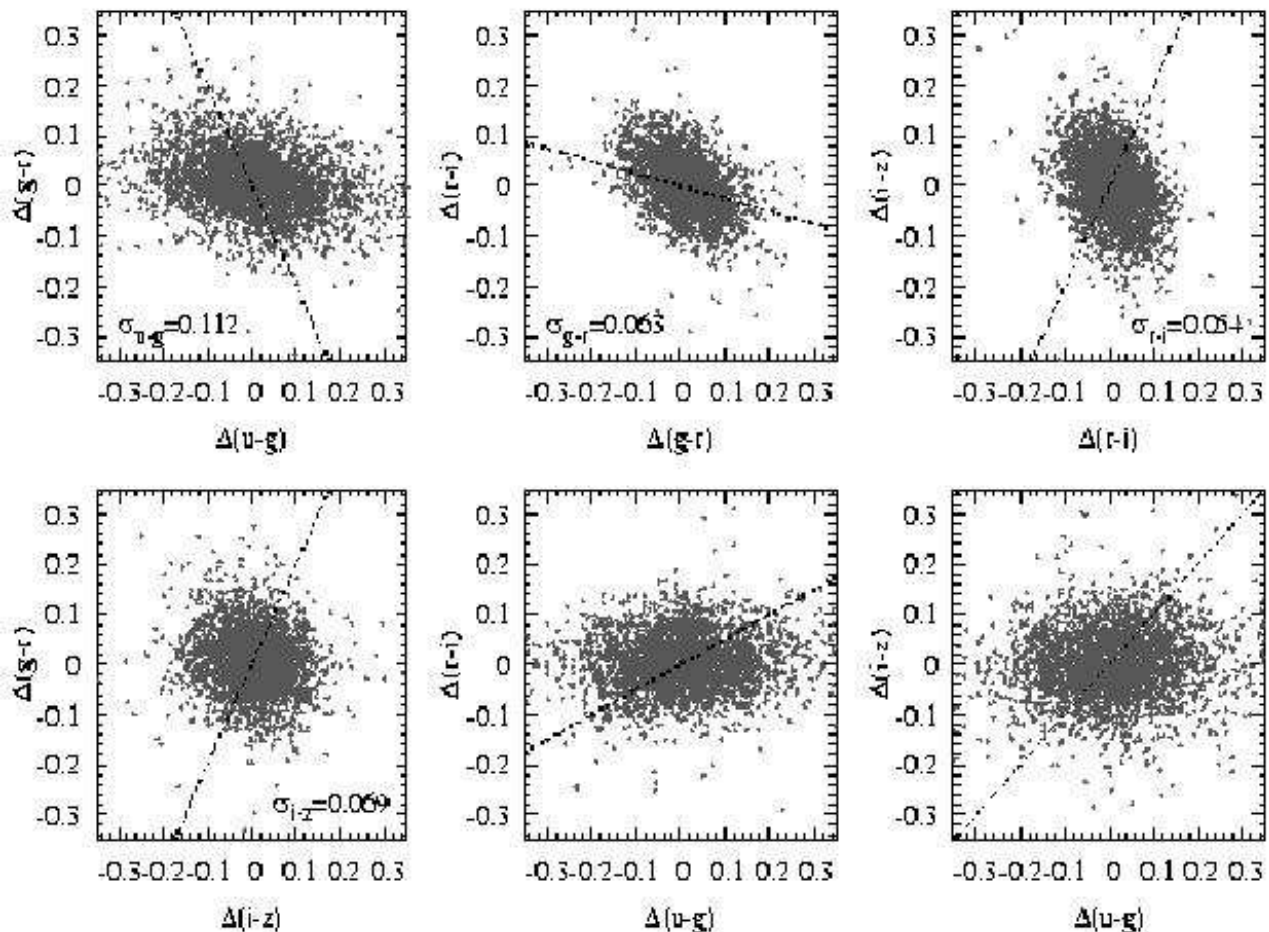


Figure 7. Correlations between the changes of four SDSS colors for the same asteroids as in Fig. 1. The dashed lines show the expected slopes if non-simultaneous observations and fast, large-amplitude variability produce significant bias in color measurements (see §3.2.4). This bias is not supported by the displayed data.

as due to mixing of the two basic materials, corresponding to C and S types, on the asteroid surfaces. We will return to this point in Section 5.

3.3 The Repeatability of Color Variations

The suite of tests in this Section suggest that the observed color variations are not an artefact (either observational, or caused by phenomena such as differential opposition effect). However the lack of any correlation with physical parameters, such as color, size and family membership, discussed in the next Section, may be elegantly explained as caused by some “hidden” random error contribution, for example a problem introduced by the processing software. Here we present a test which demonstrates that at least in one aspect the observed color variation is not random.

If it is true that asteroids exhibit a varying degree of color variability, as they do, for example, for single-band variability, then the color changes detected in two independent pairs of observations may correlate to some degree. At the same time, such a correlation would give credence to the measurements reliability. We use a subsample of 541 asteroids that were observed at least four times to test whether such a correlation exist. The top panel in Fig. 10 plots the

change of a color in a pair of observations vs. the change in another independent pair of observations. We have verified that the marginal distributions in each coordinate are indistinguishable.

To illustrate this point, in the bottom panel we compare the distributions of the a color change in one pair of observations for two subsamples selected by the a color change in the other independent pair observations, as marked by the dashed lines in the top panel. If the color changes in two pairs of observations are uncorrelated, then the two histograms should be indistinguishable. However, they are clearly different, indicating that these independent observations “know” about each other!

In order to quantify the statistical significance of the difference between the two histogram, we perform two tests. A two-sample Kolmogorov-Smirnov test (Lupton 1993) indicates that the histograms are different at a confidence level of more than 99%. Another test, proposed by Efron and Petrosian (1992), which uses the entire 2-D sample, indicates that the two variables are correlated at a confidence level of 95%. The somewhat lower confidence level than for the first test is probably due to the contribution of points with small color changes, whose distribution may be randomized by photometric errors.

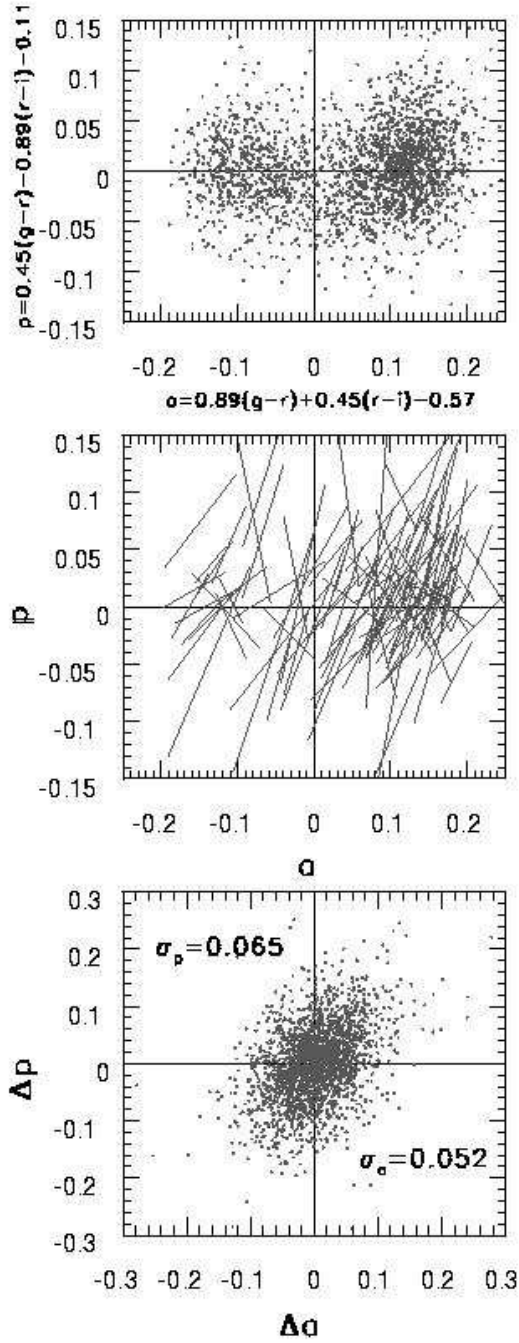


Figure 8. The top panel shows the asteroid principal color diagram, constructed with the mean colors for two measurements. In the middle panel two individual measurements are connected by lines, for a small subset of objects with $18 < r < 18.3$ and a change in each color of at least 0.03 mag. Note that for objects with large color variations, the changes of the two principal color seem to be somewhat correlated. The bottom panel show the change of p color vs. the change of a color for all the objects in the “high-quality” subsample, as well as the rms scatter in each color.

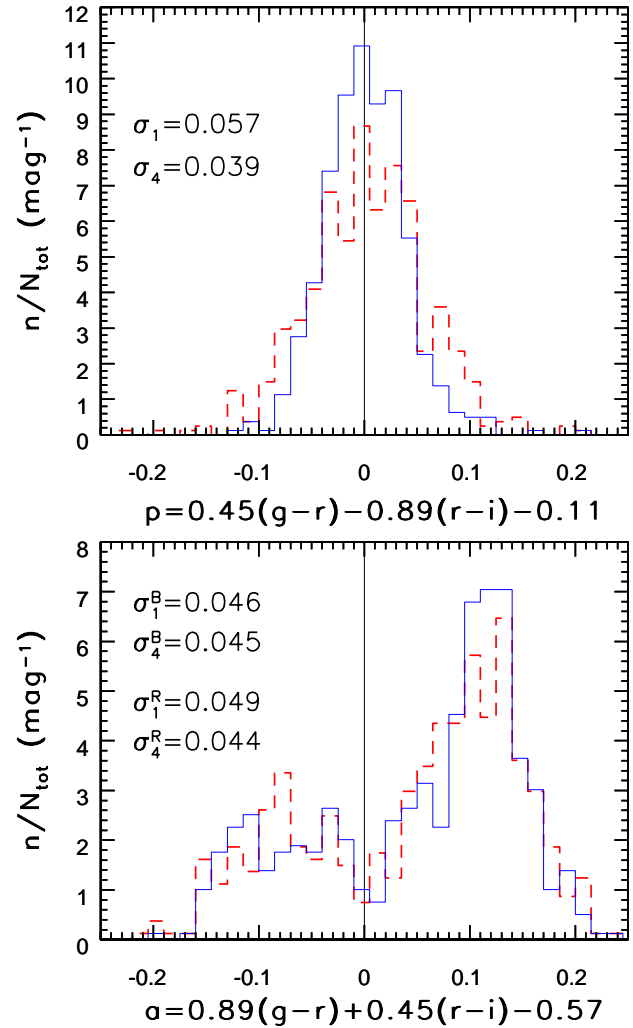


Figure 9. The comparison of the p (top panel) and a (bottom panel) color distributions obtained by averaging four measurements (solid lines) for 541 asteroids, and those for individual measurements (dashed lines). The σ values are the distribution widths, subscripted 1 for single epoch and 4 for average measurements. The widths for the a color distribution are determined separately for objects with $a < 0$ (superscripted B) and $a > 0$ (R). Note that the width of the p color distribution is 1.46 larger for single epoch measurements, while the a color distribution does not change appreciably.

We conclude that objects with large color variations in one pair of observations tend to show relatively large color variation in the other, independent, pair of observations. This difference strongly suggests that the observed color variations are real, and also indicates that for some asteroids color variations are stronger than for others.

4 THE APPARENTLY RANDOM NATURE OF COLOR VARIABILITY

A series of tests discussed in the preceding section demonstrate that the detection of asteroid color variability is robust. In this section we attempt to find correlations between

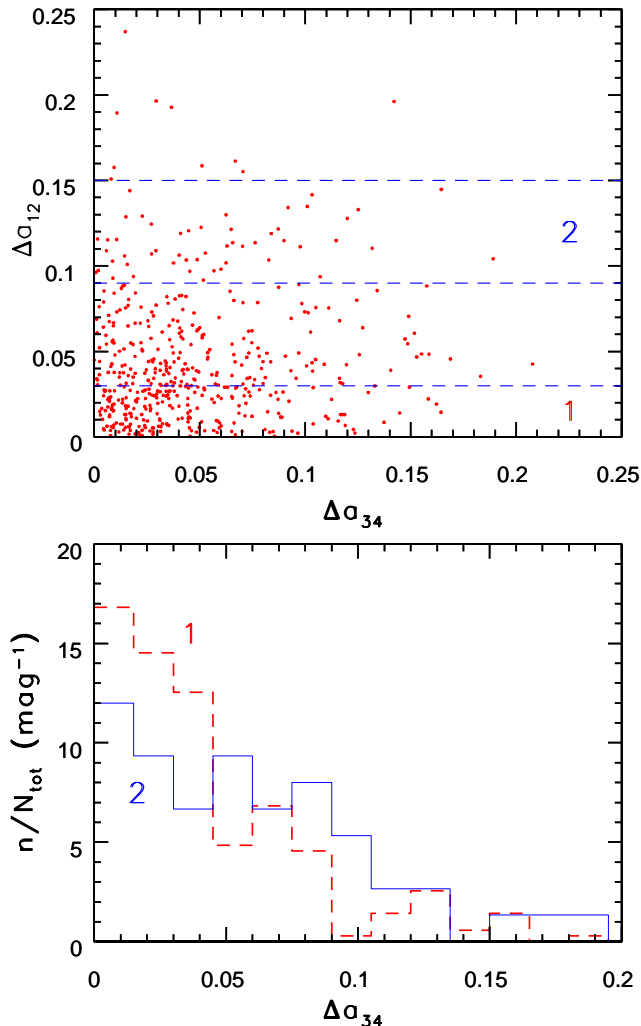


Figure 10. The top panel plots the changes of a color in two independent pairs of observations (change in the first pair vs. the change in the second pair) for 541 asteroids observed at least four times. The bottom panel compares the histograms of a color change in one of the two pairs of observations, for two subsets selected by the a color change in the other pair of observations, as marked by the dashed lines in the top panel (see text). Note that the two distributions are different, indicating that these independent observations “know” about each other. The same conclusion is obtained when the axes are reversed.

color variability and other parameters such as colors (a good proxy for taxonomic classes), absolute magnitude (i.e. size), and family membership.

4.1 Color Variability as a Function of Mean Colors

The position of an asteroid in the principal color diagram (the top panel in Fig. 8) is a good proxy for its taxonomic classification (I01). Thus, a dependence of color variability on taxonomic type would show up as a correlation between the change of a color and its mean value. We show the scatter plot of these two quantities in the upper panel in Fig. 11. The bottom panel compares the distributions of the a color

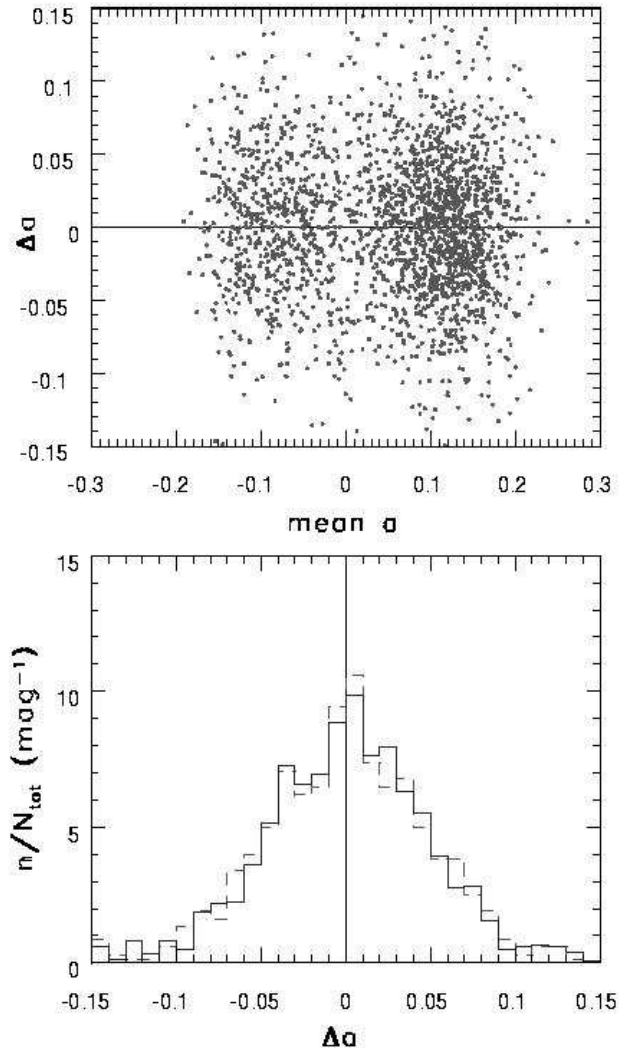


Figure 11. The upper panel shows the a color change between two epochs for the same asteroids as in Fig. 1, as a function of the mean a color. The bottom panel compares the distributions of the a color change for 689 objects with mean $a < 0$ and 1585 objects with mean $a > 0$. Note that the two histograms are statistically indistinguishable indicating that the color measurement is not correlated with the asteroid’s a color (which is a good proxy for taxonomic classification).

change for 689 objects with mean $a < 0$ (dominated by the C type objects) and 1585 objects with mean $a > 0$ (dominated by the S type objects). The two histograms are statistically indistinguishable.

While the mean-color-selected objects (blue vs. red) appear to show the same a color change distributions, it may be possible that the objects with the largest Δr or Δa would show different principal color distribution. We repeat the asteroid principal color diagram constructed with the mean colors (already shown in Fig. 8) in the top panel in Fig. 12. The same distribution is shown by linearly spaced isodensity contours in the middle and bottom panels. The dots in the middle panel represent objects with the change in the r magnitude of at least 0.2 mag. The dots in the bottom panel represent objects with the change in the a color of at least 0.05 mag. There is no discernible difference between

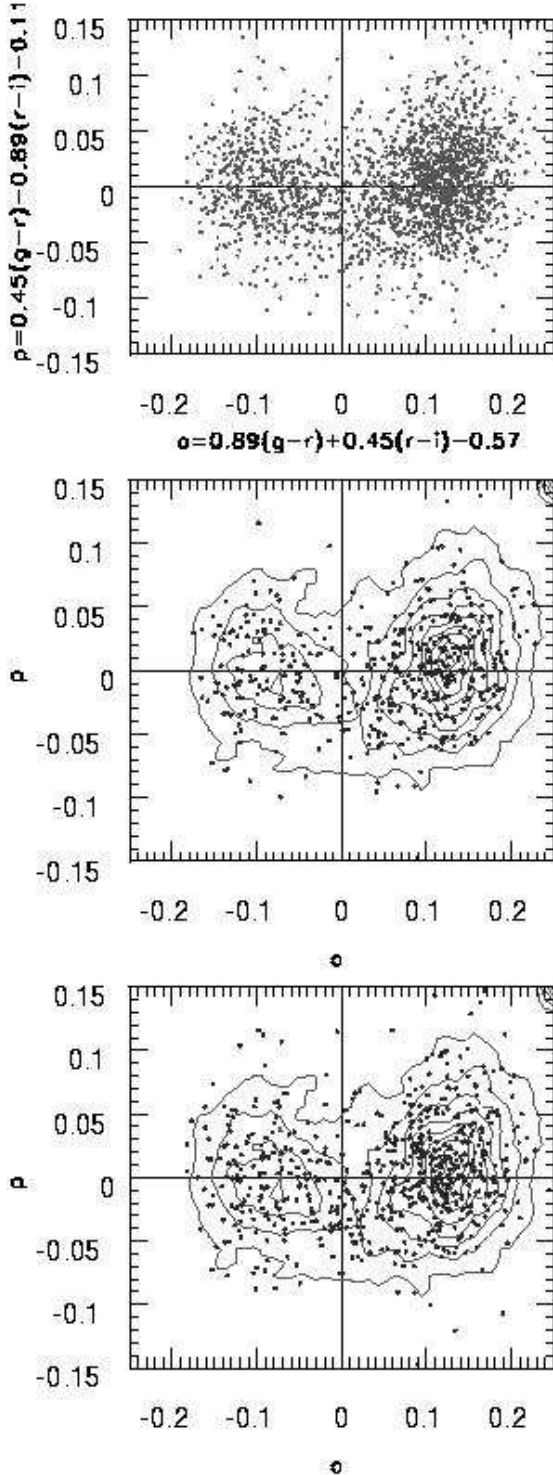


Figure 12. The top panel shows the asteroid principal color diagram, constructed with the mean colors for two measurements, for the whole sample. The same distribution is shown by linearly spaced isodensity contours in the middle and bottom panels. The dots in the middle panel represent objects with the change in the r magnitude of at least 0.2 mag. The dots in the bottom panel represent objects with the change in the a color of at least 0.05 mag. Note that objects with large changes of magnitudes and colors appear to show the same mean principal color distribution as the full sample.

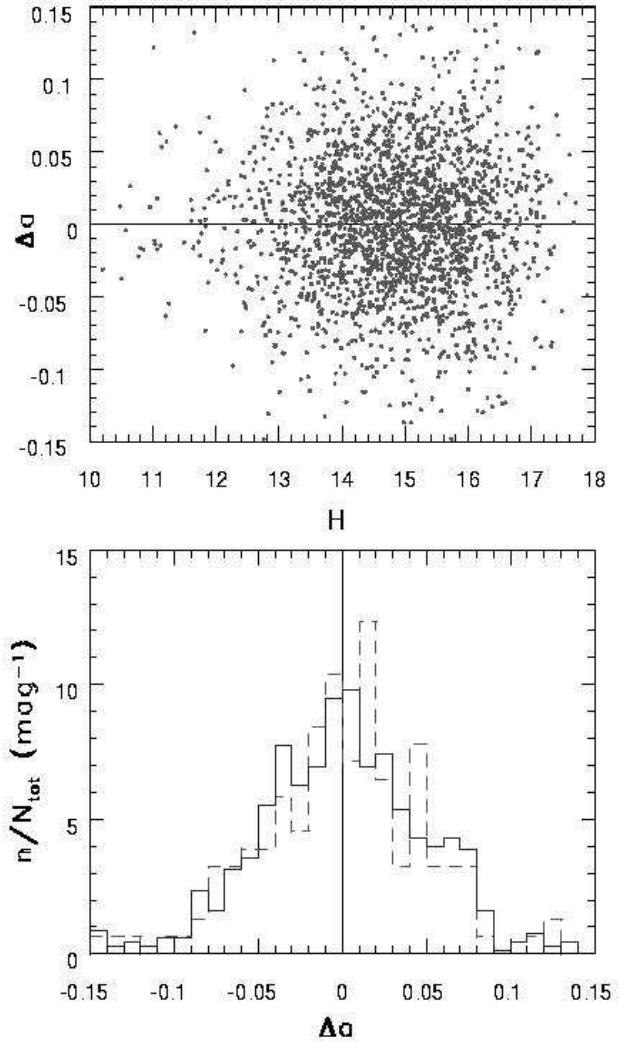


Figure 13. The upper panel shows the a color change between two epochs for the same asteroids as in Fig. 1, as a function of the absolute magnitude. The bottom panel compares the width of the distribution of the a color change for 97 objects with $10 < H < 13$ (dashed line) and for 505 objects with $15 < H < 16$ (solid line). Note that the two histograms are statistically indistinguishable indicating that the color measurement is not correlated with the asteroid's absolute magnitude (i.e. size, in the approximate range 1–10 km).

the color distribution for the whole sample and that for the highly variable objects.

4.2 Color Variability as a Function of Absolute Magnitude

Asteroids of different size may exhibit different color variability. The closest proxy for the size, in the absence of direct albedo measurements, is the absolute magnitude. Fig. 12 shows correlation between Δa and the absolute magnitude H . The displayed range of H roughly corresponds to the 1–10 km size range. The bottom panel compares the width of the Δa distribution for 97 objects with $10 < H < 13$ (dashed line) and for 505 objects with $15 < H < 16$ (solid line). The two histograms are statistically indistinguishable indicating

Table 1. The definitions of asteroid families in the a_p - $\sin(i)$ - e space

Groups	a_p	$\sin(i)$	e
Flora	2.16–2.32	0.04–0.125	0.105–0.18
Vesta	2.28–2.41	0.10–0.135	0.07–0.125
Nysa-Polana	2.305–2.48	0.03–0.06	0.13–0.21
Eunomia-Adeona	2.52–2.72	0.19–0.26	0.12–0.19
Eos	2.95–3.10	0.15–0.20	0.04–0.11
Themis	3.03–3.23	0–0.6	0.11–0.20

that the color change is not correlated with the asteroid’s absolute magnitude (i.e. size). However, we emphasize that the dynamic range of probed sizes is fairly small.

4.3 Color Variability as a Function of Family Membership

SDSS colors are a good proxy for taxonomic classification, and can be efficiently used to recognize at least three color groups (J02). I02c showed by correlating asteroid dynamical families and SDSS colors that indeed there are more than just three “shades”: many families have distinctive and uniform colors. Motivated by their finding, we obtain a more detailed classification of asteroids using dynamical clustering and correlate it with variability properties.

We define families by 3-dimensional boxes in the space spanned by proper orbital elements (the boundaries are summarized in Table 1), using the results from Zappala et al. (1995). There are 6 families with more than 50 members in the sample analyzed here. The comparison of $|\Delta a|$ and $|\Delta r|$ distributions for individual families with those for the whole sample are shown in Figs. 14 and 15, respectively. In order to quantitatively assess whether there is any family that differs in its variability properties from the rest of the sample, we performed two-sample Kolmogorov-Smirnov tests. None of the families listed in Table 1 was found to differ from the mean values for the whole sample at a confidence level greater than 95%. We conclude that all the examined families show similar variability properties.

5 DISCUSSION AND CONCLUSIONS

The detection of color variability for a large sample of asteroids discussed here represents a significant new constraint on the physical properties and evolution of these bodies. The random nature of this variability, implied by the lack of apparent correlations with asteroid properties such as mean colors, absolute magnitude and family membership, could be interpreted as due to some hidden random photometric error. However, several lines of evidence argue that this explanation is unlikely. First, the magnitude of the observed effect (0.06–0.11 mag.) is so large that such photometric errors would have to be noticed in numerous other studies and tests based on SDSS photometric data. If such an error only shows up for moving objects, then the color variability should increase with the apparent velocity, an effect which is not observed (see Fig. 2). Second, independent pairs of observations, discussed in Section 3.4, seem to “know” about each other: objects with large color variation in one pair of observations tend to show relatively large color variation in

other pair of observations. This fact cannot be explained by random photometric errors. Third, the color variation is not entirely random in the principal colors diagram, as discussed in Section 3.3. There is a preferred direction for variability-induced motion in this diagram, and the scatter in principal colors is significantly different ($\sigma_p \sim 1.33\sigma_a$). Were the color variability caused by random photometric errors, it would not be correlated with the distribution of asteroid principal colors.

The observed color variability implies inhomogeneous albedo distribution over an asteroid surface. Although the color variability is fairly small, it suggests that large patches with different color than their surroundings exist on a significant fraction of asteroids. For example, consider a limiting case of an asteroid with two different hemispheres, one with C type material, and one with S type material. In this case the peak-to-peak amplitude of its a color variability would be only 0.2 mag., with rms \sim 0.05 mag.³, even under the most favorable condition of the rotational axis perpendicular to the line of sight. Taking into account a distribution of the angle between rotational axis and the line of sight would decrease these values further. Without detailed modeling it is hard to place a lower limit on the fraction of surface with complementary color to explain the observed color variations. However, using simple toy models and colors typical for C and S type asteroids, we find that this fraction must be well over 10%. The features seen in spatially resolved color images of Eros obtained by NEAR spacecraft (Murchie et al. 2002) support such a conclusion.

A simple explanation for the existence of patches differing in color from their surroundings is the deposition of material (e.g. silicates on C type asteroids and carbonaceous material on S type asteroids) by asteroid collisions. However, such surfaces would exhibit color variations preferentially aligned with the a color axis, contrary to the observations. For a given fraction of asteroid surface affected by the deposition of new material, the large difference in albedos of silicate and carbonaceous surfaces would probably produce different amplitudes of color variability for S and C type asteroids (due to large difference in their albedos), a behavior that is not supported by the data. Thus, the color variability cannot be explained as due to patches of S-like and C-like material scattered across an asteroid surface.

A plausible cause for optically inhomogeneous surface is space weathering. This phenomenon includes the effects of bombardment by micrometeoroids, cosmic rays, solar wind and UV radiation, and may alter the chemistry of the surface material (Zeller & Rouca, 1967). Recent spacecraft data indicate that these processes may be very effective in the reddening and darkening of asteroid surface (Chapman 1996). In this interpretation the $u - g$ color should show the largest variation (Hendrix & Vilas 2003), and this is indeed supported by the data presented here (see Fig. 7). It is not clear, however, how could such processes result in fairly large isolated surface inhomogeneities.

An interesting explanation for surface inhomogeneities is the effects of cratering. Using NEAR spacecraft measurements, Clark et al. (2001) find 30-40% albedo variations on

³ The color lightcurve would be biased red because of the factor of 4 difference in the visual albedos.

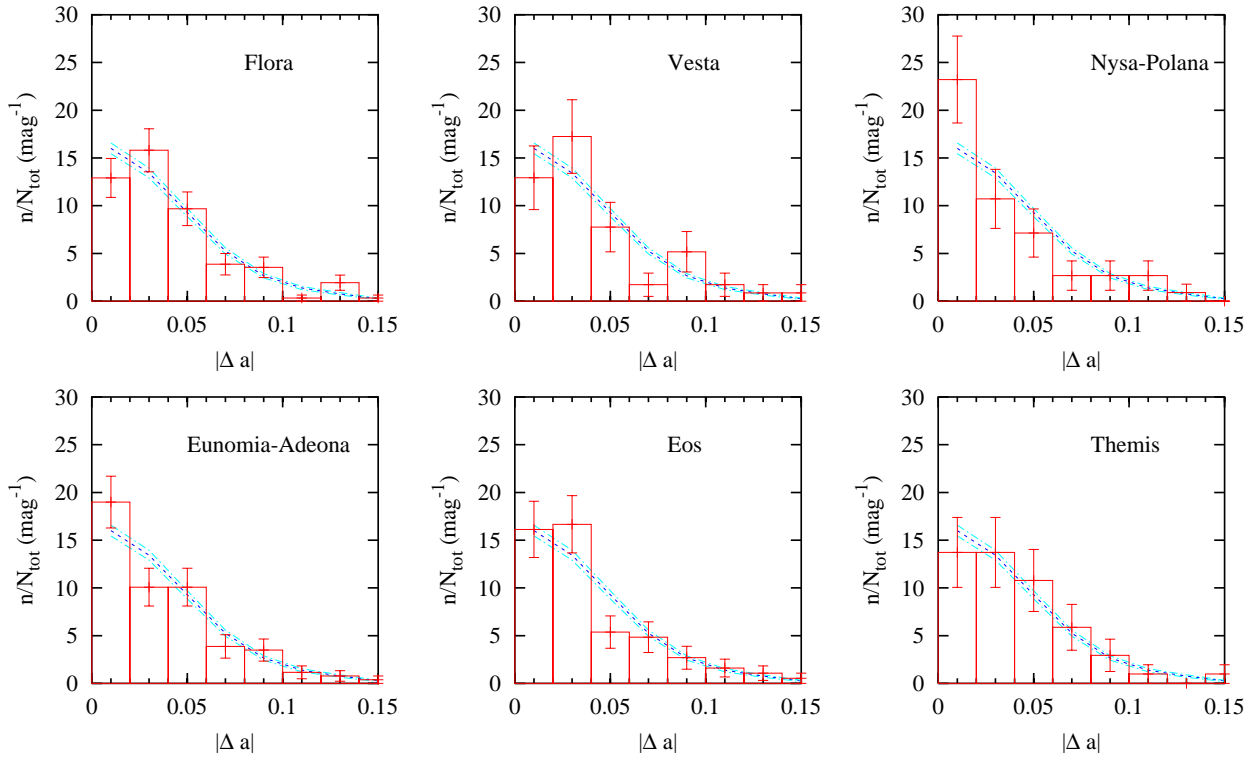


Figure 14. The distribution of $|\Delta a|$ for individual asteroid families (boxes with errorbars) is compared to the distribution for the whole sample, shown by lines (mean $\pm \sigma$). The families are defined by regions in the spaced spanned by proper orbital elements (see Table 1. and text).

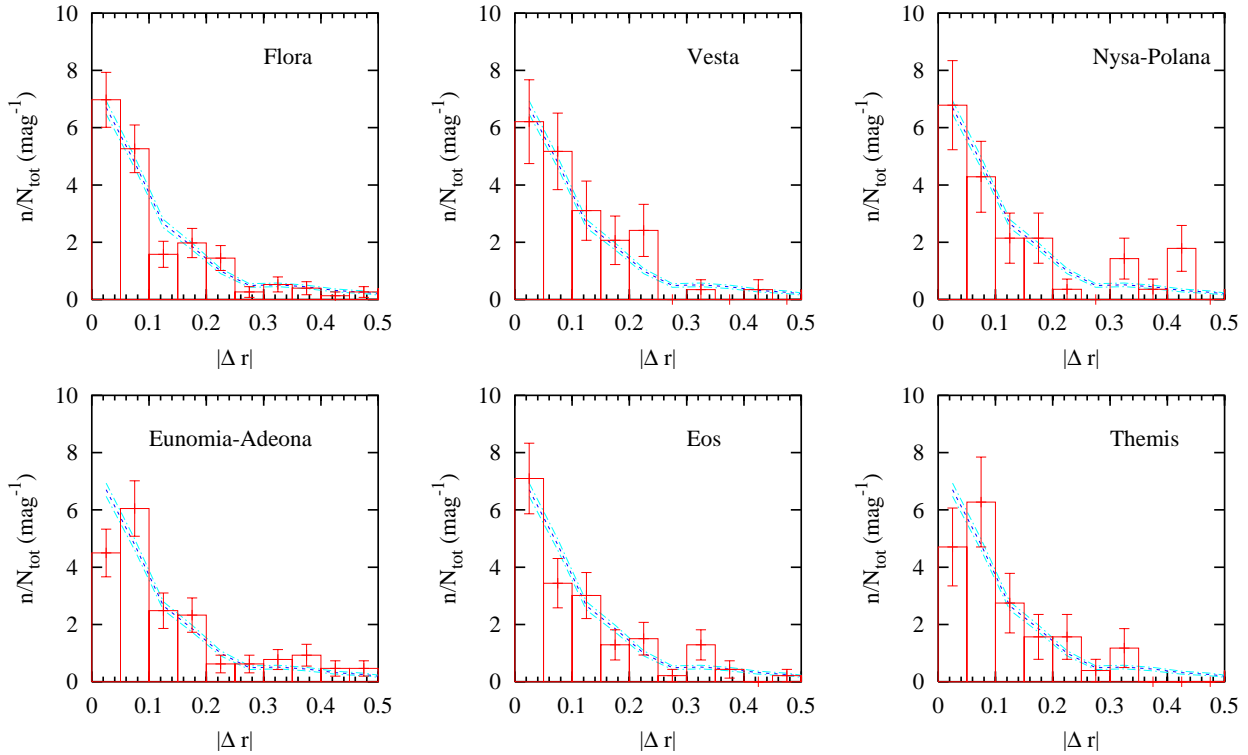


Figure 15. Same as Figure 14, except that the absolute value of the r band brightness variation is shown.

the Psyche crater wall on Eros. Such a large effect could perhaps produce color variations consistent with observations. However, it seems premature to draw conclusions with detailed modeling.

Irrespective of the mechanism(s) responsible for the observed color variations, our results indicate that this is a rather common phenomenon. We conclude by pointing out that the sample presented here will be enlarged by a factor of few in a year or two because SDSS is still collecting data, and the size of known object catalog, needed to link the observations, is also growing. Furthermore, the faint limit of the known object catalog is also improving, and will result in a larger size range probed by the sample. Apart from SDSS-MOC, the upcoming (in 5–10 years) deep synoptic surveys such as Pan-STARRs and LSST will produce samples of size and quality that will dwarf the sample discussed here, and provide additional clues about the causes of asteroid color variability.

ACKNOWLEDGMENTS

This work has been supported by the Hungarian OTKA Grants T034615, FKFP Grant 0010/2001, Szeged Observatory Foundation, and Pro Renovanda Cultura Hungariae Foundation DT 2002/maj.21. Ž.I. acknowledges generous support by Princeton University.

Funding for the creation and distribution of the SDSS Archive has been provided by the Alfred P. Sloan Foundation, the Participating Institutions, the National Aeronautics and Space Administration, the National Science Foundation, the U.S. Department of Energy, the Japanese Monbukagakusho, and the Max Planck Society. The SDSS Web site is www.sdss.org. The Participating Institutions are The University of Chicago, Fermilab, the Institute for Advanced Study, the Japan Participation Group, The Johns Hopkins University, the Max-Planck-Institute for Astronomy (MPIA), the Max-Planck-Institute for Astrophysics (MPA), New Mexico State University, Princeton University, the United States Naval Observatory, and the University of Washington.

REFERENCES

- Azebajian, K. et al., 2003, AJ, in press
 Blanco, C., Catalano, S. 1979, Icarus, 40, 359
 Binzel, R.P., et al., 1997, Icarus, 128, 95
 Bowell, E. & Lumme, K., 1979, in Asteroids, ed. T. Gehrels, (Tucson: Univ. of Arizona Press), 132
 Bowell, E. 2001, *Introduction to ASTORB*, available from <ftp://ftp.lowell.edu/pub/elgb/astorb.html>
 Chapman, C.R. 1996, Meteoritics, 31, 699
 Clark, B.E. et al. 2001, Meteoritics and Planetary Science, 36, 1617
 Degewij, J., Tedesco, E.F., Zellner, B.H. 1979, Icarus, 40, 364
 Efron, B. & Petrosian, V. 1992, ApJ, 399, 345
 Fukugita, M., et al. 1996, AJ, 111, 1748
 Gunn, J.E., et al. 1998, AJ, 116, 3040
 Hendrix, A.R., Vilas, F. 2003, 34th Annual Lunar and Planetary Science Conference, March 17-21, 2003, League City, Texas
 Ivezić, Ž., Tabachnik, S., Rafikov, R., et al. 2001, AJ, 122, 2749 (I01)
 Ivezić, Ž., Jurić, M., Lupton, R.H., et al. 2002a, Survey and Other Telescope Technologies and Discoveries, J.A. Tyson, S. Wolff, Editors, Proceedings of SPIE Vol. 4836 (2002), also astro-ph/0208099
 Ivezić, Ž., Lupton, R.H., Jurić, M., et al. 2002b, AJ 124, 2943
 Ivezić, Ž., Lupton, R.H., Anderson, S., et al. 2002c, astro-ph/0301400
 Gaffey, M.J., King, T., Hawke, B.R., 1982, Workshop on Lunar Breccias and their Meteoritic Analogs, ed. by G.J. Taylor and L.L. Wilkening, LPI, Houston
 Jurić, M., Ivezić, Ž., Lupton, R.H., et al., 2002, Astronomical Journal, 124, 1776
 Lupton, R.H., Gunn, J.E., Ivezić, Ž., et al., 2001, in *Astronomical Data Analysis Software and Systems X*, ASP Conference Proceedings, Vol.238, p. 269. Edited by F. R. Harnden, Jr., Francis A. Primini, and Harry E. Payne. San Francisco: Astronomical Society of the Pacific, ISSN: 1080-7926
 Lupton, R.H., 1993, Statistics in theory and practice, Princeton, N.J.: Princeton University Press
 Magnusson, M., 1991, A&A, 243, 512
 Melillo, F.J., 1995, MPBu 22, 42
 Metcalf, J.H., 1907, ApJ, 25, 264
 Milani, A. et al., 1999, Icarus, 137, 269
 Mottola, S., Gonano-Beurer, M., Green, S.F., et al., 1994, P&SS, 44, 21
 Murchie, S., Robinson, M., Clark, B., et al., 2002, Icarus, 155, 145
 Pravec, P., Harris, A.W., 2000, Icarus, 148, 12
 Reed, K.L., Gaffey, M.J., Lebofsky, L.A., 1997, Icarus, 125, 446
 Schober, H.J., Schroll, A., 1992, in: Sun and Planetary System, Dordrecht, D. Reidel Publishing Co., 1982, 258
 Sekiguchi, T., Boehnhardt, H., Hainaut, O. R., Delahodde, C. E., 2002, A&A, 385, 281
 Sheppard, S.S., Jewitt, D.C., 2002, AJ, 124, 1775
 Shoemaker, E., Williams, J.G., Helin, E.F., & Wolfe, R.F. 1979, in Asteroids, ed. T. Gehrels, (Tucson: Univ. of Arizona Press), 253
 Smith, J.A. et al., 2002, AJ, 123, 2121
 Stoughton, C. et al., 2002, AJ, 123, 485
 Szabó, Gy.M., Kiss, L.L., Sárneczky, K., et al., 2001, A&A 384, 702
 Thomas, P. C., Binzel, R. P., Gaffey, M. J., et al., 1997, Science, 277, 1492
 Zappala, V., Bemdjaya, Ph., Cellino, A., Farinella, P., Froeschlé, C. 1995, Icarus, 116, 291
 Zeller, E.J., Rouse, L.B., 1967, Icarus, 7, 372
 Zellner, B. 1979, in Asteroids, ed. T. Gehrels, (Tucson: Univ. of Arizona Press), 783
 Zellner, B., Tholen, D.J. & Tedesco, E.F., 1985, Icarus, 61, 355